

## Oil field microorganisms cause highly localized corrosion on chemically inhibited carbon steel

Jaspreet Mand\*  and Dennis Enning

Research & Technology Development, Upstream Integrated Solutions, ExxonMobil Upstream Research Company, Spring, TX, USA.

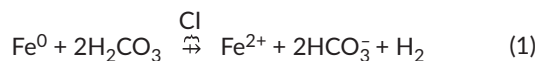
### Summary

**Carbon steel pipelines, a means for crude oil transportation, occasionally experience highly localized perforation caused by microorganisms. While microorganisms grown in laboratory culture tend to corrode steel specimens unevenly, they rarely inflict a corrosion morphology consistent with that of pipelines, where centimetre-sized corrosion features are randomly distributed within vast stretches of otherwise pristine metal surface. In this study, we observed that corrosion inhibitors (CIs), widely used for the control of acid gas (H<sub>2</sub>S, CO<sub>2</sub>) corrosion in oil fields, also affect microbial growth and activity. Inhibited carbon steel resisted biofilm formation and underwent negligible corrosion (< 0.002 mm Fe<sup>0</sup> year<sup>-1</sup>), despite 15 months of exposure to oil field waters harbouring a diverse microbiome. In contrast, physical scavenging of CI in these waters led to severe and highly localized corrosion (up to 0.93 mm Fe<sup>0</sup> year<sup>-1</sup>) underneath biofilms dominated by methanogenic archaea and sulfate-reducing bacteria. A sharp decline in CI concentration, as well as its active components, quaternary ammonium compounds (QACs), correlated with microbial sulfidogenesis. CIs are ubiquitously present in oil field waters and play an underappreciated role in microbial corrosion mitigation. Physical and biological scavenging of CIs may create local differences in steel inhibition effectiveness and thus result in highly localized corrosion.**

### Introduction

In 2018, global crude oil production exceeded 100 million barrels per day for the first time in history (U.S. Energy Information Administration, 2018). The transportation of these hydrocarbons to industrial end users (e.g. refineries) requires vast infrastructure, such as buried and above-ground pipelines. Carbon steel is the preferred manufacturing material for such pipelines, due to its excellent mechanical properties and low cost (Ahmad, 2006). However, carbon steel is also inherently prone to corrosion and the integrity of ferrous infrastructure requires careful management in order to guarantee long-term operability and to prevent the release of hazardous liquids to the environment (Ahmad, 2006).

At oil production sites, a primary means of corrosion mitigation is the use of corrosion inhibitors (CIs; Sanyal, 1981; Kermani and Morshed, 2003; Achour and Kolts, 2015). These oil field chemicals ward against the corrosive effects of the acid gases CO<sub>2</sub> and H<sub>2</sub>S, which are soluble in water and can be abundant in petroleum reservoirs (Nešić, 2007). Most CIs are surfactant-like organic molecules that chemisorb to steel and form a physical barrier between the metal and its corrosive environment (Migahed and Al-Sabagh, 2009). They owe this functional property to their molecular structure; a surface-active head group and hydrophobic aliphatic tail structure allows the CI to bind to metallic surfaces and form a persistent film that repels hydrophilic molecules (Sanyal, 1981; Migahed and Al-Sabagh, 2009). Commercially available products for inhibition of acid gas corrosion are often chemical mixtures that contain the surfactant-like active ingredient(s) blended into solvents and synergistic chemistries. Commonly used active ingredients include quaternary ammonium compounds (QACs), imidazoles, imidazolines, amines and phosphate esters (Dariva and Galio, 2014). The inhibition of CO<sub>2</sub> (carbonic acid) corrosion with CI can be depicted as follows:



While carbonic acid tends to be less problematic in waters at pH > 7 where it gets rapidly deprotonated and protective iron carbonate (FeCO<sub>3</sub>) films are more likely to develop on carbon steel surfaces, carbonic acid corrosion needs to be adequately inhibited under the (slightly)

Received 27 April, 2020; revised 10 July, 2020; accepted 18 July, 2020.

\*For correspondence. E-mail jaspreet.mand@exxonmobil.com; Tel. +1 832 624 2531.

*Microbial Biotechnology* (2021) 14(1), 171–185

doi:10.1111/1751-7915.13644

### Funding information

No funding information provided.

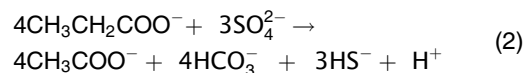
© 2020 The Authors. *Microbial Biotechnology* published by Society for Applied Microbiology and John Wiley & Sons Ltd

This is an open access article under the terms of the Creative Commons Attribution-NonCommercial-NoDerivs License, which permits use and distribution in any medium, provided the original work is properly cited, the use is non-commercial and no modifications or adaptations are made.

acidic conditions that prevail in most production systems. Typical injection rates in oil fields are 10–300 mg Cl<sup>-</sup> l<sup>-1</sup> of total fluid (crude oil + water; Palmer *et al.*, 2004).

In addition to dissolved acid gases, the oil field microbiome poses a threat to materials integrity (Duncan *et al.*, 2009; Vigneron *et al.*, 2016; Vigneron *et al.*, 2017; Fig. 1). The infrastructure used for the production, processing and transportation of crude oil teems with microbial life, and many different microorganisms have been demonstrated to affect the corrosion of steel, a phenomenon termed microbially influenced corrosion (MIC). Two physiological groups that have received particular attention in the context of MIC are the sulfate-reducing bacteria (SRB) and methanogenic archaea, owing to their prevalence in corroding infrastructure and the ability of some isolates to inflict severe metal damage in laboratory experiments (Mori *et al.*, 2010; Uchiyama *et al.*, 2010; Enning *et al.*, 2012; Enning and Garrelfs, 2014). Most crude oil-associated anoxic waters are replete with readily available organic and inorganic electron donors for anaerobic microbial metabolism (Magot *et al.*, 2000). This can be problematic if the microbial degradation of these compounds is coupled to the production of corrosive metabolites such as

reduced sulfur species (Lee *et al.*, 1995; Enning and Garrelfs, 2014; Lahme *et al.*, 2019) or nitrite (Drønen *et al.*, 2014; Lahme *et al.*, 2019). Corrosion that is caused by microbial metabolites is sometimes referred to as chemical microbially influenced corrosion (CMIC; Enning *et al.*, 2012). CMIC may, for instance, result from the incomplete oxidation of propionate by SRB and the concomitant generation of sulfide (Eq. 2), which is corrosive to steel (Eq. 3).



Another corrosion mechanism that has come to prominence in recent years is the so-called electrical microbially influenced corrosion (EMIC; Dinh *et al.*, 2004; Enning *et al.*, 2012). Some microorganisms can grow lithotrophically with metallic iron (Fe<sup>0</sup>) as their sole electron donor in laboratory experiments. These peculiar isolates of SRB and methanogenic archaea derive energy from the coupling of Fe<sup>0</sup> oxidation to the reduction of sulfate (Eq. 4) and CO<sub>2</sub> (Eq. 5), respectively.

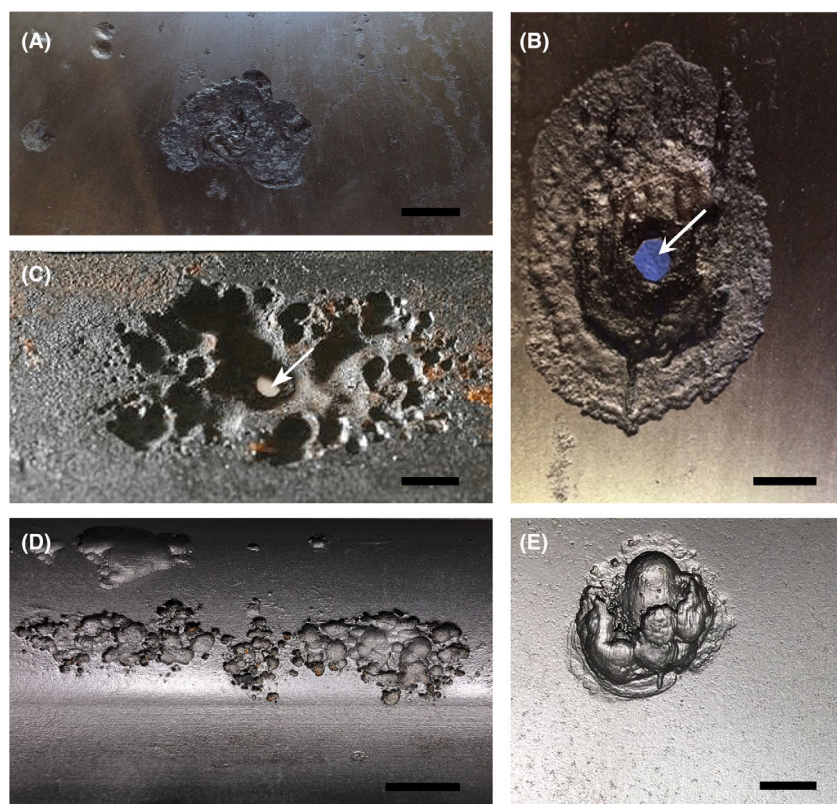
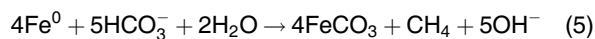
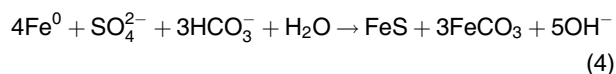


**Fig. 1.** Examples of highly localized corrosion in crude oil transmission pipelines. All images depict internal corrosion features on the bottom of carbon steel pipelines. White arrows in B and C indicate full wall penetration. A: bar = 2 cm. B: bar = 1 cm. C: bar = 1 cm. D: bar = 1 cm. E: bar = 1 cm.



The responsible microorganisms, many of which also grow on solid-state electrodes (Beese-Vasbender *et al.*, 2015a,b; Deutzmann and Spormann, 2017; Deng *et al.*, 2018), supposedly utilize iron-derived electrons for their metabolism through redox-active proteins that are in electrical short-circuit with the metal. SRB are thought to achieve this through outer membrane *c*-type cytochromes (Dinh *et al.*, 2004; Beese-Vasbender *et al.*, 2015a,b; Deng *et al.*, 2018; Tang *et al.*, 2019), while methanogenic archaea oxidize iron through extracellular hydrogenases to a similar effect (Deutzmann *et al.*, 2015; Tsurumaru *et al.*, 2018).

It is a widely held conception in the oil and gas industry that the formation of biofilms is a prerequisite for MIC (Skovhus *et al.*, 2017); hence mitigation of MIC in pipelines focuses on the removal and inactivation of steel-attached microorganisms, which is achieved through mechanical cleaning ('pigging') and periodic biocide application, respectively. Intriguingly, microbial corrosion tends to be highly localized in carbon steel pipelines, particularly in those that are downstream of processing facilities which remove much of the oil-associated natural gas (including CO<sub>2</sub>) and water. Microorganisms typically corrode steel specimens unevenly (Enning *et al.*, 2012) and may cause micrometre-scale pitting in laboratory experiments (Starosvetsky *et al.*, 2000; Chen *et al.*, 2015a,b). However, such studies come short at explaining the patchy occurrence of MIC in actual pipelines, where millimetre- to centimetre-sized localized corrosion features are found within swathes of otherwise virtually pristine metal surface (see Fig. 1 for examples).

Corrosion inhibitors (CIs) have received little attention in the context of MIC, despite their ubiquity in crude oil production, transportation and storage facilities (Duncan *et al.*, 2014). We speculated that CIs, which are surface-active and toxic, have a major yet widely overlooked impact on oil field biofilm formation and MIC. We therefore studied the effects of CI on biofilm ecology, microbial activity and corrosion in laboratory experiments with produced waters and microorganisms from West African oil field pipelines.

## Results and discussion

### *Corrosion inhibitors influence biofilm formation and MIC in West African produced water*

As produced water gravity separates from crude oil in transmission systems, MIC is usually observed at the steel–water interface along the bottom of pipelines.

While the settled water can contact vast stretches of metal, the occurrence of metal damage tends to be highly localized and at seemingly random locations (Fig. 1). We suspected that CIs, which are amply used in crude oil production facilities for the inhibition of acid gas corrosion, coincidentally also influence the extent and morphology of MIC. To test this hypothesis, we collected oil and associated produced water from a production site in West Africa which uses CI and has a documented history of microbial corrosion (Keasler *et al.*, 2010). Once received at the laboratory, oily anoxic produced water was separated and transferred into nine butyl rubber-stoppered 1 l glass bottles containing vertically mounted corrosion coupons (microcosms, Fig. S1). This water contained a residual CI concentration of 3–5 mg l<sup>-1</sup> in the bulk liquid. In order to study the effect of CI on biofilm formation and corrosion, we lowered the concentration of CI in a sub-set of the microcosms by adding sterilized laboratory-grade sand to five of the nine bottles. Sand is known to adsorb CI in oil field settings (Horsup *et al.*, 2007) and effectively lowered CI concentrations in this study (Fig. S2). The two sub-sets of microcosms developed markedly different appearances over the course of the 15 months experiment. While there was no physical contact between the mounted steel coupons and the added sand that accumulated on the glass bottoms, metal coupons started blackening within weeks and were covered in millimetre thick, dark deposits by the end of the experiment. By contrast, steel coupons in the unaltered (no sand) microcosms remained clean and of metallic appearance during the entire 15 months. Further analysis of the steel specimens unveiled profound differences in metal integrity (Figs 2A and S3). Deep and highly localized corrosion features were observed on coupons from microcosms with sand (Fig. S3), which had a lowered residual CI concentration of  $1.2 \pm 0.6 \text{ mg l}^{-1}$  ( $n = 5$ ). Interpolated pitting (localized) corrosion rates in these bottles averaged  $0.33 \pm 0.07 \text{ mm Fe}^0 \text{ year}^{-1}$  ( $n = 15$ ), and rates as high as  $0.93 \text{ mm Fe}^0 \text{ year}^{-1}$  were observed on some coupons (Fig. 2C). Microbial corrosion of this magnitude would reduce the service life of a typical carbon steel pipeline to less than 10 years. By contrast, there was no pitting corrosion on coupons in the unaltered (no sand) bottles with higher residual CI concentrations ( $3.1 \pm 0.4 \text{ mg l}^{-1}$ ;  $n = 4$ ). In addition, Fe<sup>0</sup> weight loss was negligible ( $0.0018 \pm 0.0004 \text{ mm Fe}^0 \text{ year}^{-1}$ ;  $n = 12$ ) and almost 50 times lower than in bottles with sand ( $0.088 \pm 0.021 \text{ mm Fe}^0 \text{ year}^{-1}$ ,  $n = 15$ , Fig. 2C).

The observed differences in corrosion called for the analysis of biofilms that had developed under the respective conditions with and without CI scavenging. Intriguingly, there was little biomass on steel coupons in bottles without sand (high CI); these biofilms contained

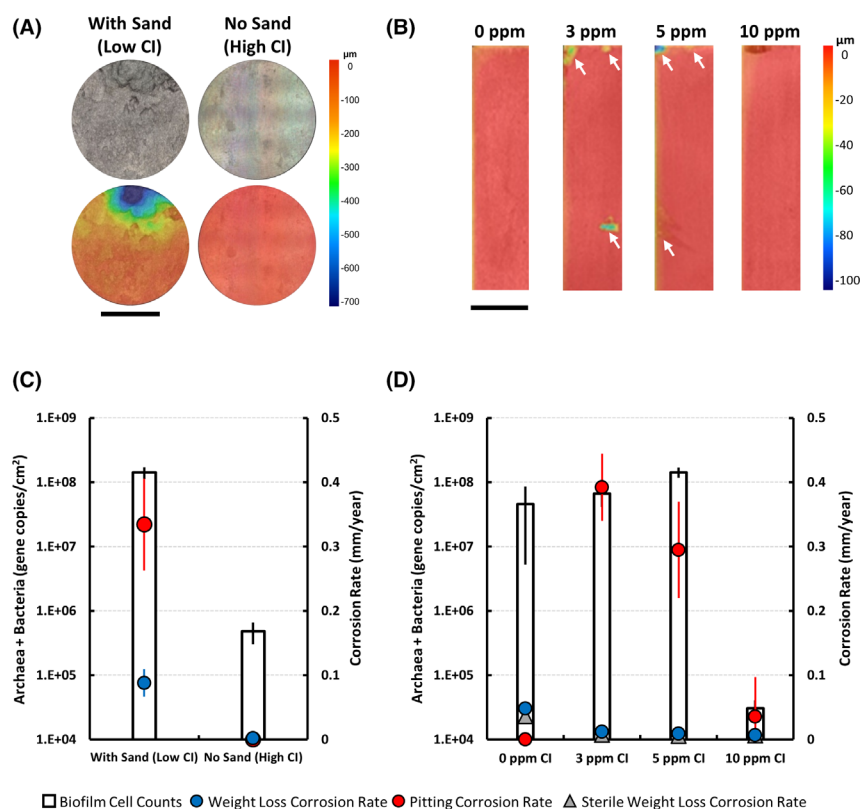


**Fig. 2.** Highly localized corrosion of carbon steel coupons in laboratory experiments with oily produced water or synthetic produced water medium containing oil field microorganisms.

A. Photographs (top row) and surface depth profile (bottom row) of cleaned corrosion coupons exposed to anoxic oily produced water (PW) for 15 months. One set of coupons ( $n = 15$ ) was incubated in microcosms containing PW in which corrosion inhibitor (CI) concentrations had been lowered through sand addition. Another set of coupons ( $n = 12$ ) was incubated in PW containing residual CI. One representative coupon is shown for each condition. Bar = 1 cm.

B. Corrosion coupons exposed for 3 months to oil-free, synthetic produced water medium containing different concentrations of CI ( $n = 3$  for each condition). Depth profiles for  $\frac{1}{4}$  of the surface of one representative coupon per condition are shown. Bar = 1.25 cm. White arrows denote localized corrosion features.

C. Interpolated annualized weight loss-based and localized profilometry-based corrosion rates in produced water cultures ( $n = 15$  with sand,  $n = 12$  without sand), along with corresponding biofilm cell count ( $n = 5$  with sand,  $n = 4$  without sand).

D. Extrapolated annualized weight loss-based and localized corrosion rates in synthetic produced water medium containing different concentrations of CI, along with corresponding biofilm cell count ( $n = 3$ ). Extrapolated annualized weight loss-based corrosion rates in sterile synthetic produced water medium are also shown ( $n = 1$ ).

100 times fewer bacterial and archaeal 16S rRNA gene copies  $\text{cm}^{-2}$  than biofilms grown in bottles with sand (Fig. 2C). The residual concentration of surface-active CI in the West African produced water had apparently hindered biofilm formation on tested steel specimens over more than one year in laboratory studies. The observed differences in biofilm formation were particularly interesting as there was no distinct effect of CI on planktonic

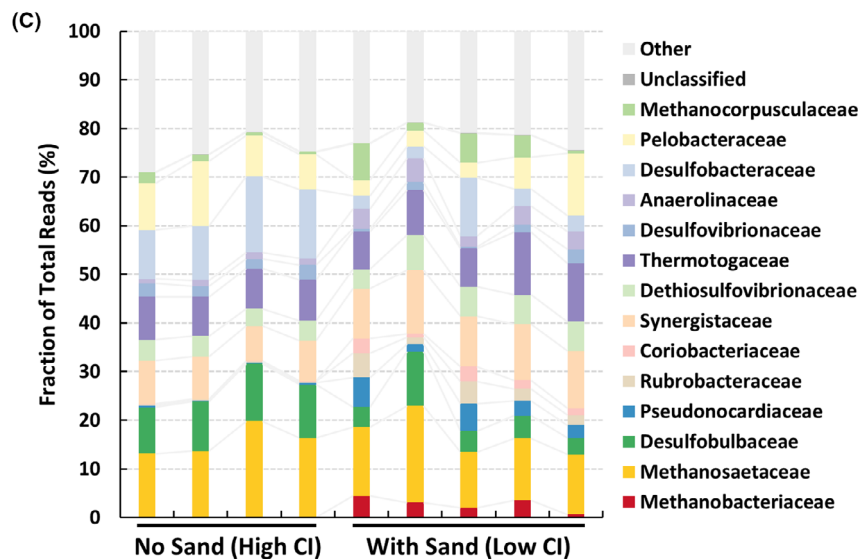
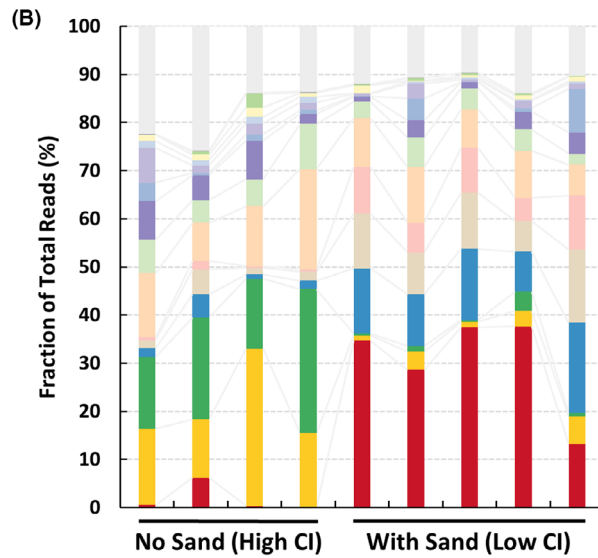
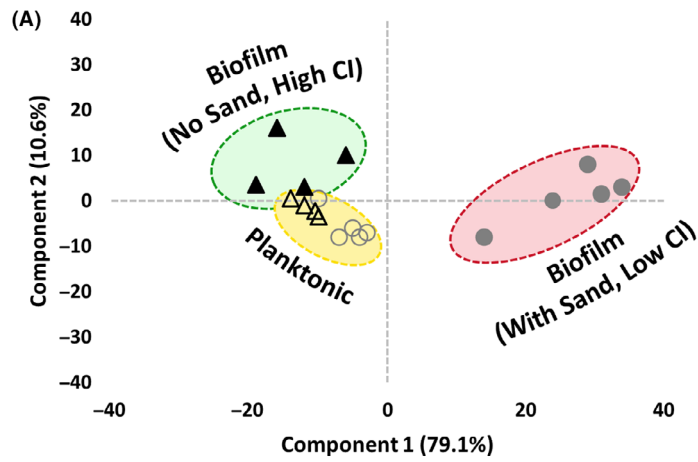
cell numbers in the two sets of microcosms (Fig. S4A). The numbers of planktonic microorganisms were in fact comparable in all bottles ( $4.4 \times 10^6 - 1.7 \times 10^7$  gene copies  $\text{ml}^{-1}$ ), i.e. unaffected by CI concentration in the bulk fluid. As negatively charged steel surfaces attract the positively charged surfactant-type CIs, it is expected that CIs are more aggregated and present at higher volumetric concentrations in the direct vicinity of the metal

**Fig. 3.** Steel-attached biofilm and planktonic microbial communities in anoxic microcosms with oily produced water and carbon steel coupons at the end of the 15 months experiment. One set of microcosms ( $n = 4$ ) was incubated without sand, with produced water still containing  $3.1 \pm 0.4 \text{ mg Cl l}^{-1}$  at test end. In the other set of microcosms ( $n = 5$ ), residual CI concentrations had been lowered through addition of sand to  $1.2 \pm 0.6 \text{ mg l}^{-1}$ .

A. Principal component analysis of microbial community composition in steel-attached biofilms (sessile) and free produced water (planktonic).

B. Sessile bacterial and archaeal microbial community composition of biofilms collected from steel coupons.

C. Planktonic bacterial and archaeal microbial community composition in microcosm produced waters. (B) and (C) depict families which account for  $\geq 2.5\%$  of total reads (average of biological replicates) in at least one of the four data sets (sand, no sand, sessile, planktonic).



compared to the bulk fluids (Zhu *et al.*, 2017). This may explain the profound differences between biofilm and planktonic cell viability in cultures without sand.

Furthermore, 16S rDNA amplicon sequencing revealed similarities in planktonic microbial community composition between the nine microcosms at the end of the experiment regardless of CI concentration (Fig. 3A and C). Steel-attached biofilms in incubations with lowered CI concentrations, on the other hand, were dominated by markedly different microorganisms (Fig. 3A and B). Archaeal *Methanobacteriaceae* accounted for  $30.3 \pm 3.4\%$  of the microbial population covering corroded steel surfaces (with sand, low CI), but were only minor community members ( $1.8 \pm 1.5\%$ ) of the overall less abundant biofilm on uncorroded coupons (no sand, high CI). It is tempting to speculate that these steel-attached archaea may have caused much of the observed metal damage. Recently, the genome of one species within the *Methanobacteriaceae* was shown to encode a corrosive extracellular [NiFe]-hydrogenase (Tsurumaru *et al.*, 2018), while other strains have been found to rapidly corrode  $\text{Fe}^0$  (according to Eq. 5) in laboratory experiments (Dinh *et al.*, 2004). In this experiment,  $\text{Fe}^0$  served as a solid-state electron donor and may have enriched for sessile microorganisms that are capable of an  $\text{Fe}^0$ -based metabolism. However, steel-derived electrons remained inaccessible in the set of microcosms that contained higher concentrations of CI. Only a small number of microorganisms attached to the chemically inhibited steel ( $4.8 \times 10^5 \pm 1.6 \times 10^5$  gene copies  $\text{cm}^{-2}$ ), and these microorganisms resembled the microbial makeup of the produced water (Figs 2C and 3A–C). Members of the *Methanosaetaceae* and *Desulfobulbaceae*, for instance, can degrade acetate and propionate which were present in the West African produced waters at the start of the experiment, and so these microorganisms may have relied on these soluble electron donors for their growth (Widdel and Pfennig, 1982; Smith and Ingram-Smith, 2007). Steel-attached biofilms in incubations with low CI (with sand) also contained *Pseudonocardiaceae*, *Rubrobacteraceae* and *Coriobacteraceae*. Members of these *Actinobacteria* groups have been found to utilize various hydrocarbons as carbon and energy sources in petroleum-containing environments and may have been using residual hydrocarbon associated with the produced water in this experiment (Kotani *et al.*, 2006; Chen *et al.*, 2015a,b).

Only few studies have probed the influence of CIs on oil field microorganisms and have primarily focused on product toxicity (Choi *et al.*, 2002; Liu *et al.*, 2016). Duncan *et al.* (2014) studied corrosion in sulfidogenic oil field cultures in once-flow-through bioreactors and first documented an observed impact of CI on pitting of carbon steel. We hypothesized that CIs can inhibit MIC and

offer two mechanistic explanations for our observations. First, the film-forming CIs protected steel effectively against the corrosive metabolite sulfide (e.g. from the metabolism of *Desulfobulbus* sp.; see Eqs. 2 and 3), and hence mitigated CMIC. Second, CIs exhibited a surface toxicity effect that prevented the growth of steel-attached corrosive microorganisms capable of EMIC, such as *Methanobacterium* sp. In microcosms where sand had been added to physically scavenge some of the CI, chemical inhibition was reduced in its effectiveness and highly localized corrosion on otherwise pristine steel surfaces resulted from insufficient chemical protection (Figs 2A and S3). However, while adequately simulating oil field MIC, the use of oily produced water and physical scavenging of CI may have potentially introduced experimental artefacts that complicate the interpretation of our results. We therefore investigated the activity of oil field microorganisms in the presence of CI under more defined conditions, using synthetic growth media.

#### *Under-dosing of CI led to microbially influenced, highly localized corrosion on carbon steel*

In order to further study the impact of CI on microbial activity, we incubated steel specimens in microcosms with synthetic produced water medium for three months. This medium was modelled after the West African produced water, but contained only acetate (12.1 mM) and propionate (1.6 mM) as organic electron donors. Triplicate 2 l microcosms containing carbon steel coupons were amended with CI at 0, 3, 5 and 10  $\text{mg l}^{-1}$  and inoculated with an enrichment culture from the oil field. These experimental conditions were selected to model concentrations of CI previously observed in bottle tests with actual produced waters. The commercial CI which was used in the West African oil field and in this laboratory study, contains quaternary ammonium compounds (QACs) with hydrophobic aliphatic chain lengths between  $\text{C}_{12}$  and  $\text{C}_{16}$ . Besides their use in CIs, QACs find application as organic disinfectants in other industries and are, for example widely used in consumer care products (Tezel and Pavlostathis, 2015). QACs are cationic surfactants that owe their antimicrobial properties to the disruption of a cell's physical and ionic stability (Wessels and Ingmer, 2013). Indeed, we confirmed that as little as 3  $\text{mg l}^{-1}$  of this QAC-containing CI effectively prevented sulfidogenesis and methanogenesis in  $\text{Fe}^0$ -free planktonic cultures of the oil field enrichment (Fig. S5). The response in  $\text{Fe}^0$ -containing microcosms, on the other hand, was different. Steel-attached biofilm grew despite the addition of 3  $\text{mg l}^{-1}$  or 5  $\text{mg l}^{-1}$  CI and reached comparable cell counts as the CI-free control ( $4.6 \times 10^7 \pm 4.0 \times 10^7$  gene copies  $\text{cm}^{-2}$ ; Fig. 2D). Furthermore, biofilms grown in synthetic produced water

medium with 3 mg l<sup>-1</sup> or 5 mg l<sup>-1</sup> CI contained similar numbers of microorganisms as biofilms grown in actual produced water with lowered CI concentration (sand addition; compare Fig. 2C and D). Addition of 10 mg CI l<sup>-1</sup>, however, profoundly limited formation of biofilm ( $3.1 \times 10^4 \pm 1.0 \times 10^4$  gene copies cm<sup>-2</sup>). Chemical inhibition reduced both, abiotic and microbially influenced oxidation of Fe<sup>0</sup>, with at least threefold lower coupon weight loss observed in microcosms with CI compared to the CI-free controls (Fig. 2D). Overall, the formation of biofilm on steel coupons in these tests only moderately increased coupon weight loss compared to sterile controls (an increase of 33–75%). However, this microbially influenced increase in corrosion occurred in a highly localized manner on chemically inhibited steel surfaces in cultures with a starting concentration of 3 mg l<sup>-1</sup> or 5 mg l<sup>-1</sup> CI (Fig. 2B). Technically relevant localized metal damage was observed on these coupons, and corrosion rates ( $0.39 \pm 0.05$  mm Fe<sup>0</sup> year<sup>-1</sup>; Fig. 2D) were in fact comparable to those in long-term produced water incubations with lower CI concentrations (Fig. 2C). We attributed the highly localized corrosion to microbial activity, as control incubations with CI under sterile conditions were devoid of such corrosion features (Fig. S6).

Addition of CI effectively diminished corrosion and the formation of molecular hydrogen in sterile control incubations (Eq. 1, Figs 2D and S7B). Despite reaching similar biofilm cell counts by the end of the experiment, microbial activity throughout the experiment was affected by the addition of CI at 3 mg l<sup>-1</sup> or 5 mg l<sup>-1</sup>. Addition of these chemicals delayed microbial sulfate reduction and methanogenesis, as well as the microbial oxidation of H<sub>2</sub>, propionate and acetate compared to CI-free controls (Fig. S8). The delay may be best explained by an impediment of microbial metabolism due to sublethal concentrations of the added organic disinfectants. The inhibitory effect of QACs on methanogenic archaea in wastewater treatment plants and biogas reactors has been observed elsewhere (Garcia *et al.*, 1999; Tezel *et al.*, 2006). At 10 mg CI l<sup>-1</sup>, microbial activity was reduced to a minimum and only apparent from the consumption of small quantities of cathodic hydrogen (from Eq. 1; Fig. S7A).

Biofilms were largely composed of sulfate-reducing *Desulfovibrionaceae* and *Desulfobulbaceae*, along with a number of facultatively anaerobic microorganisms within the families *Pseudomonadaceae*, *Bacillaceae* and *Deferribacteraceae* (Fig. S9A). The synthetic produced water further contained large proportions of *Desulfobacteraceae* and *Methanosaetaceae* in several of the incubations (Fig. S9B). We did not, however, observe in any of these incubations members of the *Methanobacteriaceae*, for which we had previously speculated an involvement in EMIC and which were abundant in tests with actual

produced water (Fig. 3). The detection of delta-proteobacterial SRB and acetoclastic methanogens (*Methanosaetaceae*) was consistent with the observed consumption and production patterns of propionate, acetate, sulfide and methane (Fig. S8A–D). The role of other detected microorganisms was less apparent and could not be inferred from the monitored metabolites.

#### *Oil field microorganisms influence the performance and concentration of corrosion inhibitors*

Laboratory testing with synthetic produced water and the West African enrichment culture supported our hypothesis that certain CIs can prevent biofilm formation and MIC on carbon steel. Additionally, we were able to reproduce the observation that inhibited carbon steel can become subject to highly localized microbial corrosion if an insufficient quantity of CI is present. In the absence of CI, the oil field culture rapidly performed incomplete oxidation of propionate and reduced sulfate (according to Eq. 2; Fig. S8A–C). The resultant sulfide reacted with steel (Eq. 3) and/or precipitated with ferrous iron from CO<sub>2</sub> corrosion (Eq. 1) as FeS, and dissolved sulfide concentrations declined steadily over the course of the experiment (Fig. 4A). We attributed the observed incremental metal loss in the presence of the oil field microorganisms to CMIC, as the detected quantities of sulfide (up to 0.6 mM) were sufficient to explain the surplus of iron oxidation (according to Eq. 3), compared to sulfide-free sterile controls. The onset of sulfidogenesis was delayed in incubations with 3 mg l<sup>-1</sup> or 5 mg l<sup>-1</sup> CI, and sulfide concentrations remained steady during the course of the experiment due to the chemical inhibition of (biogenic) H<sub>2</sub>S corrosion (Fig. 4B and C). Intriguingly, CI concentrations declined in these microcosms, a phenomenon that was not observed in sterile controls and was, as such, attributed to microbial activity. The decline in detectable CI in triplicate microcosms coincided precisely with the onset of sulfide formation in these cultures (Fig. 4B and C, shaded areas). Our CI detection methodology is based on the formation of a chloroform-soluble, coloured complex between methyl orange and cationic surfactants (such as QACs; Wang and Langley, 1975). We excluded both, an interference of dissolved sulfide with the assay and a reaction of dissolved sulfide with CI as potential explanations for this observation. CI concentrations remained steady in sterile laboratory experiments containing sulfide (Fig. S10A), with minor decreases in CI concentrations best explained through formation of CI-binding iron sulfide particles from traces of dissolved iron (7.5 µM) in the culture medium. Negatively charged surfaces such as those generated through precipitation of FeS would be expected to bind cationic surfactants and thereby reduce detectable CI concentrations. It is conceivable that biogenic H<sub>2</sub>S from

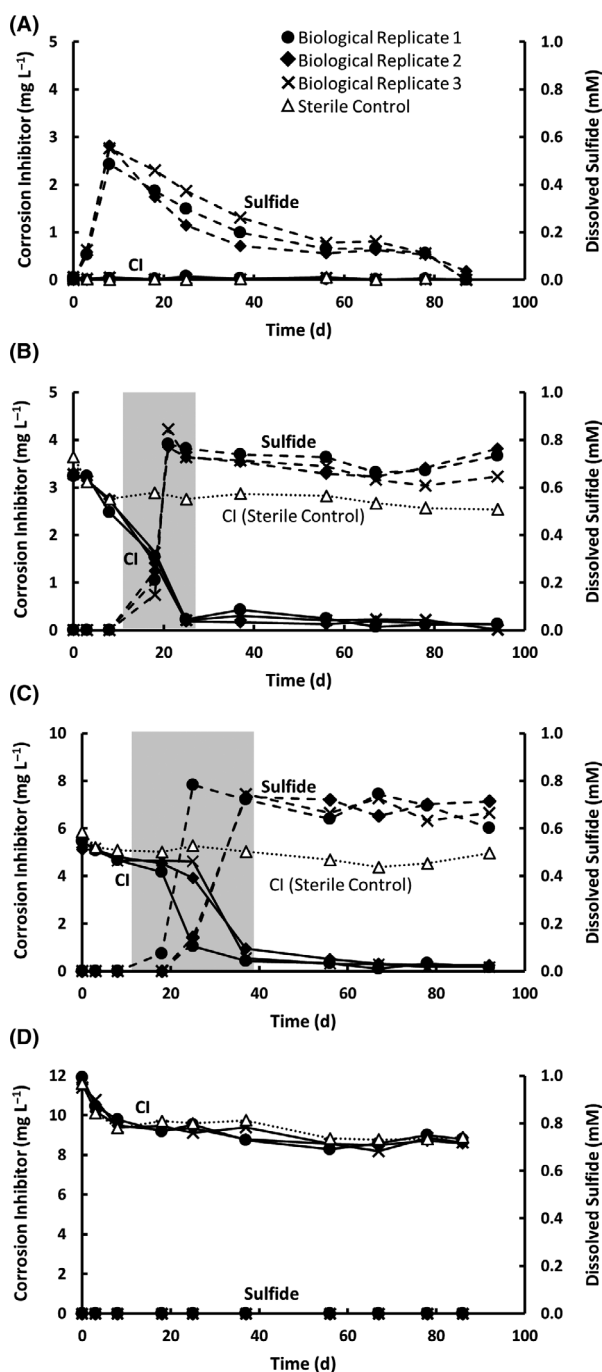


**Fig. 4.** Dissolved sulfide (dashed lines) and corrosion inhibitor (CI) concentration (bold lines) in biological triplicate cultures of oil field microorganisms in synthetic produced water medium containing carbon steel coupons. CI concentration in sterile controls is also shown. Sulfide was not detected in any of the sterile controls (data not plotted).

A. CI-free control cultures.

B. Cultures with addition of 3 mg CI l<sup>-1</sup> at test start.

C. Cultures with addition of 5 mg CI l<sup>-1</sup> at test start.

D. Cultures with addition of 10 mg CI l<sup>-1</sup> at test start. Shaded areas in (B) and (C) highlight sulfidogenesis and biologically mediated decrease of CI concentration in these actively growing oil field cultures.

planktonically grown SRB caused the highly localized corrosion on insufficiently inhibited steel (i.e. at 3 mg l<sup>-1</sup> or 5 mg l<sup>-1</sup> CI) and that the resultant larger quantities of FeS particles (from Eq. 3) adsorbed CI in these incubations. This may have then paved the way for microbial attachment and growth of sessile microorganisms, thereby further exacerbating MIC. Alternatively, SRB might have influenced CI concentrations more directly. We observed a decline of CI concentrations also in Fe<sup>0</sup>-free anaerobic incubations (Fig. S10A), and QACs may have been hydrolysed or sequestered by this sulfidogenic oil field enrichment culture. The anaerobic degradation of QACs is believed to be a slow process in natural and engineered environments (Zhang *et al.*, 2015). On the other hand, it may be worth considering that this enrichment culture has been obtained from an oil field with continuous exposure to this particular chemical over years, and as such may have adapted. Under aerobic conditions, degradation of QACs can be swift and *Pseudomonas* spp. play a prominent role as they perform the chemical activation and  $\beta$ -oxidation of the aliphatic side chains (Tezel and Pavlostathis, 2015). When added to an oxygenated artificial seawater medium with a marine inoculum, we observed biological degradation of 20 mg l<sup>-1</sup> of this CI within just 3 weeks (Fig. S11). Pseudomonads are commonly observed in oil fields (Li *et al.*, 2014; Vigneron *et al.*, 2016) and were also detectable in our mixed microbial communities (Fig. S9), but their potential involvement in the observed drop of CI concentration remains elusive as neither oxygen nor nitrate was present as electron acceptor for these facultatively anaerobic microorganisms in our experiments.

In order to evaluate if also individual, commonly used active ingredients of CIs are affected by microorganisms in a similar manner as the tested chemical cocktail, we conducted experiments with benzyldimethyl-*n*-dodecylammonium chloride (a C<sub>12</sub>-QAC) and benzyldimethyl-*n*-hexadecylammonium chloride (a C<sub>16</sub>-QAC). In experiments with 2 mg l<sup>-1</sup> of the C<sub>12</sub>-QAC, its concentration decreased and became undetectable within three weeks in the presence of steel coupons and the oil field enrichment culture (Fig. S12A). Similarly, the concentration of C<sub>16</sub>-QAC dropped below that of a sterile control, albeit not to zero, within the test duration (Fig. S12B). It is possible that the increased chain length of C<sub>16</sub>-QAC made it less biodegradable (Garcia *et al.*, 1999). Again, localized MIC was observed on inhibited steel, yet only in one of the two duplicate cultures with C<sub>12</sub>-QAC (Fig. S12C).

#### *Towards an understanding of oil field biofilm formation and MIC on chemically inhibited steel*

The formation of biofilm on metallic surfaces can lead to corrosion (Fig. 5A). In crude oil transmission pipelines,

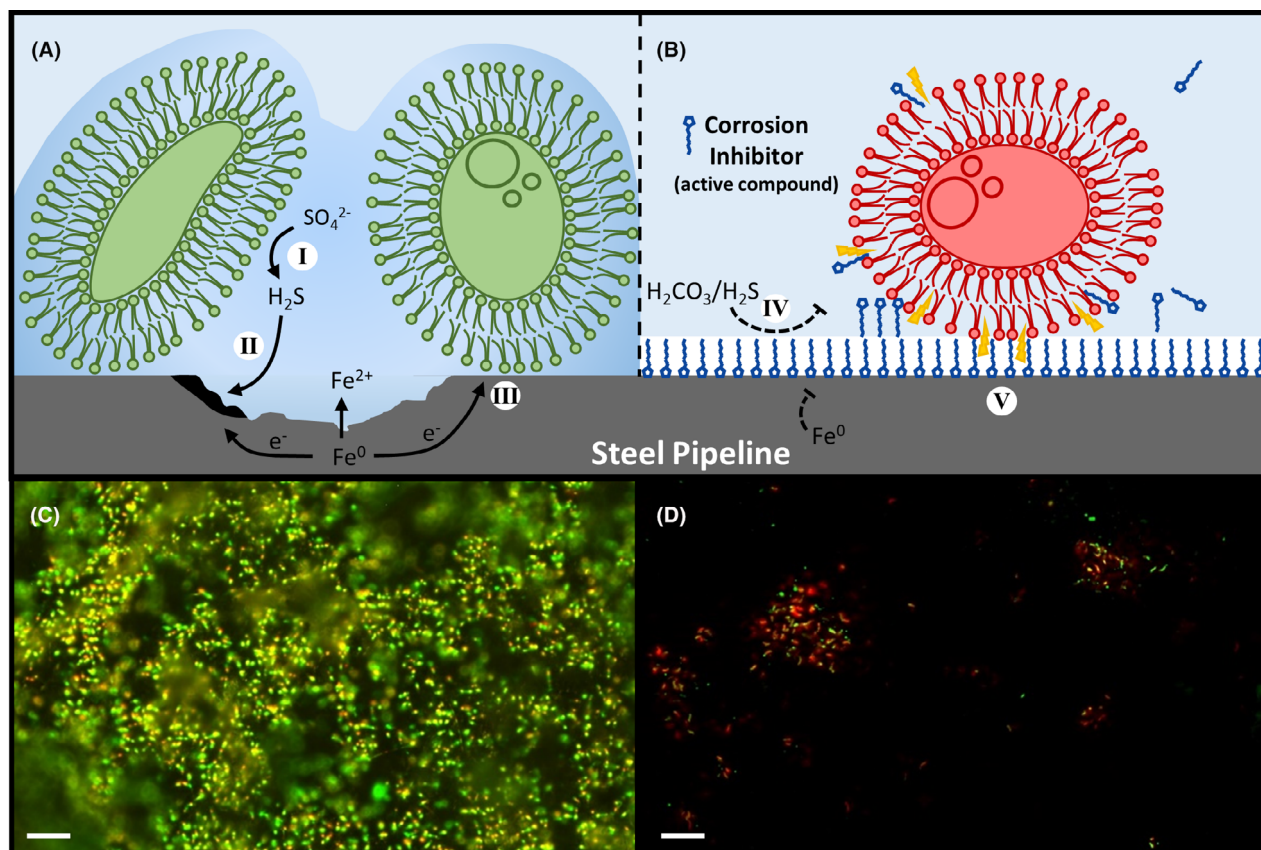


**Fig. 5.** Schematic model for the proposed impact of corrosion inhibitors (CIs) on oil field biofilm formation and MIC (A, B) and epifluorescent micrographs of corresponding examples of steel-attached biofilm (C, D). A. Oil field biofilm on carbon steel in the absence of CI. Metal damage may result from the microbial production of metabolites such as  $\text{H}_2\text{S}$  (I; compare Eq. 2), which is corrosive to steel (II; compare Eq. 3). In addition, microbial corrosion can be more direct and involve the microbial utilization of iron-derived electrons (III; compare Eqs. 4 and 5). B. CIs can limit biofilm formation and protect against MIC. A CI layer inhibits corrosion by carbonic acid and biogenic  $\text{H}_2\text{S}$  (IV; compare Eqs. 1 and 3). CI further disrupts cell membrane integrity, thereby limiting microbial attachment and growth (V) and any direct (EMIC) or indirect (CMIC) corrosion that may result from biofilm activity. C. Epifluorescence micrograph of oil field biofilm grown on steel in the absence of CI. D. Epifluorescence micrograph of oil field biofilm grown on chemically inhibited carbon steel in the presence of  $10 \text{ mg CI l}^{-1}$ . Both biofilms were stained with SYTO9<sup>®</sup> and propidium iodine to differentiate cells with compromised membrane integrity (red) from viable microorganisms (green). Representative images were chosen from steel-attached biofilm grown in triplicate cultures with synthetic produced water medium. Scale bar =  $10 \mu\text{m}$ .

such MIC tends to occur in a highly localized manner (Fig. 1). The reasons for the occurrence of randomly distributed corrosion features on otherwise uncorroded steel surfaces, however, have remained enigmatic. In this study, we produced evidence that CIs can confer long-term protection of carbon steel through prevention of biofilm formation and protection against corrosive metabolites, such as  $\text{H}_2\text{S}$  (Fig. 5B IV and V). QAC-containing CIs affect microbial metabolism in a concentration-dependent manner. While at high concentrations QACs are toxic to microbial life, their mode of action at sublethal concentrations is complicated and includes multiple processes such as loss of membrane osmoregulation, dissipation of the proton-motive force, inhibition of respiratory enzymes as well as oxidative stress which can ultimately

lead to mutations and gene transfers (Tezel and Pavlostathis, 2015). We observed retarded microbial growth at concentrations of  $3 \text{ mg l}^{-1}$  or  $5 \text{ mg l}^{-1}$  of this particular QAC-containing CI (Figs 4 and S8A–D). At higher concentrations, CI can form an apparently impenetrable layer on carbon steel that prohibits microbial colonization of the metallic substratum through disruption of cell membrane functionality (Fig. 5B V). The effect of CI on cellular metabolism and viability may be particularly pronounced for microorganisms at the steel–water interface, as this is where CI concentrations will be highest (Zhu *et al.*, 2017). We used biofilm staining with the fluorescent dyes SYTO9<sup>®</sup> and propidium iodine to visualize that the membrane integrity of microorganisms attached to chemically inhibited steel was in fact compromised

(Fig. 5C and D). CIs impact the oil field microbiome, and can in extreme cases profoundly limit the ability of microorganisms to attach to carbon steel surfaces within the vast oil production and transportation infrastructure (Fig. 5B and D).

It is conceivable that inhibited and un-inhibited steel surfaces coexist in the same pipeline, thereby explaining local differences in corrosion. Analysis of biofilm from a corroded crude oil transmission pipeline in North America supported this assumption (Fig. 1B). The corrosion feature in the 6 o'clock position of this pipeline contained mature biofilm ( $3.1 \times 10^8$  16S rRNA gene copies  $\text{cm}^{-2}$ ), while there were three orders of magnitude fewer cells ( $2.4 \times 10^5$  16S rRNA gene copies  $\text{cm}^{-2}$ ) on the virtually uncorroded pipeline surface in its immediate proximity. These numbers were in fact remarkably similar to those observed in our long-term laboratory tests with actual and synthetic West African produced waters (Fig. 2C and D). It is currently unknown whether the occurrence of localized MIC on chemically inhibited carbon steel is truly random. The initiation of pitting corrosion by acid gases on chemically inhibited steel has been attributed to local differences in metal microstructure (Hayden *et al.*, 2019), and this may also apply to microbiological instances of corrosion (Walsh *et al.*, 1993). However, highly localized MIC on chemically inhibited carbon steel in pipelines may also be explained through heterogeneous sand deposition which may locally scavenge CI (Pandarinathan *et al.*, 2013; compare also Fig. S2) and thereby initiate MIC underneath these deposits. Corrosion under deposits is widely observed in oil fields and has in some instances been linked to MIC (Vera *et al.*, 2012). Crude oil transmission pipelines could be particularly prone to the effects of MIC on chemically inhibited steel. First, MIC is typically the predominant internal corrosion mechanism as corrosive acid gases have largely been removed from these systems through processing and tank storage. Second, crude oil transmission pipelines are often operated under intermittent flow conditions where stagnant periods might allow for the accumulation of biogenic sulfide and the settling of sand and other particles.

## Conclusions and outlook

The oil field microbiome is heavily affected by specialty chemicals which are widely used in the oil and gas industry for integrity management. The most prominent example in this context are biocides, which are injected for the very purpose of controlling microbial activity. Globally, 151 000 metric tons of organic biocides were used in 2017 to prevent or reduce the deleterious effects of environmental microorganisms in oil field operations (Beraud *et al.*, 2018). On the other hand, CIs are injected in even larger volumes (404 000 metric tons in

the same year), yet their role in microbial control and MIC has remained understudied and is often entirely overlooked in operational settings. In this study, we have shown that QAC-containing CIs can severely impede oil field biofilm formation and MIC under some conditions, while their use may lead to highly localized microbial corrosion in other instances where insufficient CI is available. CIs are pervasive in crude oil production, transportation and storage, and further research is needed to better understand and predict the influence of these integrity chemicals on the ecology and physiology of oil field microorganisms, particularly in the context of MIC.

## Experimental procedures

### *Produced water sampling and laboratory incubation*

Produced fluids (crude oil, water and associated gas) were collected in 5-gallon steel drums lined with an inert material at an oil-producing asset offshore Nigeria on 24 March 2016. Drums were capped to maintain anaerobic conditions and shipped to the United States at ambient temperature. In the laboratory, oily produced water (PW) was separated from crude oil through gravity separation and anaerobically transferred into 9 glass bottles (1 l, filled with 500 ml PW at pH 6.6) under a headspace of 21% (vol/vol)  $\text{CO}_2$  and 79% (vol/vol)  $\text{N}_2$  ( $\text{CO}_2\text{-N}_2$ ) (Table S2). Each bottle was amended with an anaerobic sterile 1M solution of  $\text{Na}_2\text{SO}_4$  to reach a final concentration of 4.2 mM sulfate. In each microcosm, 3 carbon steel coupons (X52 grade carbon steel; exposed surface area =  $1.25 \text{ cm}^2$  per coupon) were suspended vertically using an inert polyetheretherketone (PEEK) coupon holder, as described elsewhere (Fig. S1; Lahme *et al.*, 2019). Sterilized sand (15 % wt/vol, Carbo Ceramics, Carbo Northern White™, 30/50 mesh) was added to 5 of the 9 microcosms. All microcosms were incubated for 15 months at 32°C on a clockwise-rotating shaker (75 r.p.m.) to allow for microbial growth and the study of MIC.

### *Laboratory incubations with synthetic produced water medium*

To study the impact of CI under defined conditions, tests were set up with synthetic produced water medium, which was modelled after the West African field water chemistry (Table S2). The medium (1.6 l) contained (in  $\text{g l}^{-1}$  water) NaCl (15.31),  $\text{MgCl}_2 \cdot 6\text{H}_2\text{O}$  (0.562),  $\text{CaCl}_2 \cdot 2\text{H}_2\text{O}$  (0.434), KCl (0.121),  $\text{Na}_2\text{SO}_4$  (1.48), NaBr (0.064),  $\text{NaCH}_3\text{CO}_2$  (0.996) and  $\text{NaC}_3\text{H}_5\text{O}_2$  (0.157). Following transfer into 2 l glass bottles, the medium was purged with  $\text{CO}_2\text{-N}_2$ , sealed with a butyl rubber stopper and autoclaved. Once cooled, a sterile, anoxic stock solution (24.03 ml/1 l medium) of  $\text{NaHCO}_3$  (1 M, equilibrated with pure  $\text{CO}_2$ ) was added. A vitamin mixture,

trace elements, selenite–tungstate, phosphate, ammonium, vitamin B12, thiamine and riboflavin solutions (1 ml each per l of medium), prepared as described previously (Widdel and Bak, 1992), were added. Final pH of medium was between 6.5 and 6.8. One coupon (X52 grade carbon steel; 10 × 2.5 × 0.6 cm) was added to each bottle. This larger coupon size was used to better visualize macroscopic localized corrosion features surrounded by uncorroded metal surface. Five sides of each coupon had been sealed with a Teflon-based coating (Impreglon 800), so only one face of the coupon (2.5 × 10 cm) was exposed to the anoxic medium. Varying concentrations of a commercial CI formulation, ranging from 0 to 50 mg Cl I<sup>-1</sup>, were added. According to the safety data sheet (SDS) of the proprietary CI formulation, it contained 30–60% (wt/wt) methanol, 1–5% (wt/wt) isopropanol, 5–10% (wt/wt) organic sulfur-containing compounds and 16–45% (wt/wt) of a total of three different quaternary ammonium compounds (QACs). The microcosms were inoculated with 1% (vol/vol) of a produced water enrichment culture (please see Supporting Information) and incubated for 3 months at 32°C on a rotatig shaker (75 r.p.m.).

#### CI residual measurement

CI in samples (10 ml) was measured using a Filming Amine (aliphatic amines) Test Kit (CHEMetrics, Midland, VA), according to the manufacturer's instructions. Calibration curves for the colourimetric assays were generated using the proprietary CI formulation directly, or by using the model compounds benzyldimethyl-*n*-dodecylammonium chloride (C<sub>12</sub>-QAC; Sigma-Aldrich) and benzyldimethyl-*n*-hexadecylammonium chloride (C<sub>16</sub>-QAC; Sigma-Aldrich) dissolved in ultrapure water (18.2 MΩ·cm). Absorbance of the chloroform-soluble colour complex was measured at 436 nm using a Thermo Scientific Genesys 10S UV-Vis spectrophotometer.

#### Dissolved sulfide measurements

Dissolved sulfide was determined as described elsewhere (Cord-Ruwisch, 1985) with some modifications. In brief, samples (500 µl) were filtered (0.2 µm) to remove precipitated particulate sulfides, added to 10 ml of an acidic copper sulfate solution (5 mM CuSO<sub>4</sub> in 50 mM HCl) and thoroughly mixed. The absorbance of colloidal CuS was measured immediately at 480 nm using a Thermo Scientific Genesys 10S UV-Vis spectrophotometer.

#### qPCR and 16S rRNA gene amplicon sequencing

Planktonic cells in culture medium or produced water (20 ml or 60 ml) were collected on Sterivex filters

(0.2 µm) and stored at –80°C until analysis. Corrosion coupons were removed using sterile forceps and rinsed with sterile phosphate-buffered saline (PBS) solution. Biofilms were sampled using sterile swabs (minimum of 2 per coupon) and frozen at –80°C. For coupons with a surface area of 1.25 cm<sup>2</sup>, the entire coupon was sampled, whereas for larger coupons, only ¼ of the surface area (6.25 cm<sup>2</sup>) was sampled. All frozen samples were shipped on ice to Microbial Insights (Knoxville, TN) for DNA extraction. DNA was extracted using the DNA Power Soil Total DNA Isolation kits (MO BIO Laboratories, Solana Beach, CA) according to manufacturer's instructions.

Quantification of total eubacteria was performed on a QuantStudio 12K Flex Real-Time PCR System (Applied Biosystems, Grand Island, NY) using PCR primers and TaqMan probes targeting highly conserved regions (V9) of bacterial 16S rRNA genes based on primers described previously (Suzuki *et al.*, 2000). Primers to enumerate archaeal 16S rRNA genes were developed by Microbial Insights based on previously published primer sets targeting the V5-V9 regions (Yu *et al.*, 2005). All qPCR experiments included appropriate negative (no DNA) and positive control reactions. No amplification was detected in negative controls (*Ct* > total cycles).

16S rDNA libraries were generated by GENEWIZ (South Plainfield, NJ) using its proprietary 16S MetaVx™ amplification primers, PCR conditions and other library preparation protocols. Briefly, DNA was quantified using a Qubit 2.0 Fluorometer (Invitrogen, Carlsbad, CA) and DNA quality was assessed on a 0.6% agarose gel. Sequencing libraries were constructed using a MetaVx™ 16S rDNA Library Preparation kit (GENEWIZ). Generated amplicons covered the V3–V5 hypervariable regions of the 16S rRNA gene. Indexed adapters were added to the ends of these amplicons by limited cycle PCR. Sequencing libraries were validated using a DNA chip for the Agilent 2100 Bioanalyzer (Agilent Technologies, Palo Alto, CA) and quantified with the Qubit Fluorometer and real-time PCR (Applied Biosystems, Carlsbad, CA). DNA libraries were multiplexed and loaded on an Illumina MiSeq instrument according to manufacturer's instructions (Illumina, San Diego, CA). Sequencing was performed using a 2 × 250 paired-end configuration. Image analysis and base calling were conducted by the MiSeq Control Software on the MiSeq instrument. Initial taxonomy analysis was carried out on Illumina Basespace cloud computing platform.

The QIIME data analysis package was used for 16S rRNA data analysis (Caporaso *et al.*, 2010). Forward and reverse reads were joined and assigned to samples based on barcodes and then truncated by cutting off the barcode and primer sequence. Quality filtering on joined sequences was performed, and sequences that did not

fulfil the following criteria were discarded: sequence length < 200 bp, no ambiguous bases, mean quality score  $\leq 20$ . Sequences were compared with the Ribosomal Database Program (RDP) Gold Database (Cole *et al.*, 2014), using the UCHIME algorithm ([https://drive5.com/uchime/uchime\\_download.html](https://drive5.com/uchime/uchime_download.html)) to detect chimeric sequences. Once chimeric sequences were removed, the remaining sequences, ranging from 29 424 to 1 331 654 reads, were subjected to subsequent analyses. Sequences were grouped into operational taxonomic units (OTUs) using the clustering program VSEARCH (1.9.6), using the Silva 119 database (Quast *et al.*, 2012) pre-clustered at 97% sequence identity. The RDP classifier was used to assign taxonomic categories to all OTUs at confidence thresholds of 0.8. The RDP classifier uses the Silva 119 database which has taxonomic categories predicted to the species level. To evaluate how well each of these OTUs cluster, JMP Pro 14 was used to perform a principal components analysis using pairwise estimation of proportion normalized reads.

#### Data availability

The 16S rRNA gene amplicon sequencing data have been submitted to the NCBI short read archive (SRA) under the BioProject PRJNA606091.

#### Weight loss corrosion rate determination

Carbon steel coupons were sequentially sonicated in hexane, acetone and methanol (5 min each), dried in a stream of air and placed under vacuum overnight. Coupons were weighed thrice using an analytical balance, sterilized in ethanol (10 min for biotic tests; 30 min for abiotic tests) and dried under a stream of filtered N<sub>2</sub> gas prior to addition to the microcosms.

Following incubation, coupons were cleaned of corrosion products and other deposits in a warm (70°C) HCl solution (1.8 N) containing 2% propargyl alcohol (one min), neutralized in a saturated calcium hydroxide solution (30 s), scrubbed using a non-scratching nylon brush and rinsed in deionized water (Enning *et al.*, 2016). This cleaning process was repeated before coupons were rinsed in acetone and dried in a stream of air. Coupons were placed under vacuum overnight to ensure complete drying, weighed three times using an analytical balance, and the weight loss (Table S1) was converted into a general corrosion rate normalized to the exposed coupon surface and assuming a steel density of 7.87 g cm<sup>-3</sup>.

#### Localized corrosion analyses

The surface topography of cleaned coupons was mapped using a Keyence VR-3000K Wide-Area 3D

profile measuring microscope. Localized corrosion features ( $\geq 25 \mu\text{m}$  deep) were quantified by comparison with an external standard and the deepest feature, with reference to the original (pre-corrosion) z-plane for each coupon was converted into an annualized pitting corrosion rate through linear extra- or interpolation.

#### Biofilm staining and imaging

Corrosion coupons covered with biofilm were rinsed with sterile PBS to remove planktonic cells and were then transferred to sterile glass petri dishes. A working solution of fluorescent dyes was made by mixing SYTO9<sup>®</sup> and propidium iodide (LIVE/DEAD<sup>™</sup> BacLight<sup>®</sup> Bacterial Viability Kit, ThermoFisher Scientific) in 1/3 strength PBS. This dye solution was added to 1/4 of the coupon surface area (6.25 cm<sup>2</sup>) and incubated at room temperature for 20 min in the dark. Subsequently, the glass petri dish was filled with 1/3 strength PBS until the liquid level was 1 cm above the surface of the coupon. The biofilm on the coupon was imaged using a Zeiss Axio Imager.Z2m Live Cell Instrument MagLevit<sup>®</sup> with water lenses and equipped with an X-cite series 120 Q lamp (Lumen Dynamics).

#### Acknowledgements

We would like to thank Ramsey J. Smith and John Longwell for technical assistance as well as Fang Cao, Yao Xiong, David Fischer and Conchita Mendez for valuable discussion.

#### Conflict of interest

The authors declare no conflict of interest.

#### References

- Achour, M., and Kolts, J. (2015) Corrosion control by inhibition. Part I: Corrosion control by film forming inhibitors. NACE Corrosion Conference & Expo Paper no. 5475.
- Ahmad, Z. (2006) *Principles of corrosion engineering and corrosion control*. Burlington, MA: Elsevier.
- Beese-Vasbender, P.F., Grote, J.P., Garrelfs, J., Stratmann, M., and Mayrhofer, K.J. (2015a) Selective microbial electrosynthesis of methane by a pure culture of a marine lithoautotrophic archaeon. *Bioelectrochemistry* **102**: 50–55.
- Beese-Vasbender, P.F., Nayak, S., Erbe, A., Stratmann, M., and Mayrhofer, K.J.J. (2015b) Electrochemical characterization of direct electron uptake in electrical microbially influenced corrosion of iron by the lithoautotrophic SRB *Desulfopila corrodens* strain IS4. *Electrochim. Acta* **167**: 321–329.
- Beraud, S.S.L., Gao, A., and Davis, S. (2018) Oil Field Chemicals. IHS Markit<sup>™</sup>.
- Caporaso, G.J., Kuczynski, J., Stombaugh, J., Bittinger, K., Bushman, F.D., Costello, E.K., *et al.* (2010) QIIME allows

- analysis of high-throughput community sequencing data. *Nat Methods* **7**: 335–336.
- Chen, Y., Tang, Q., Senko, J.M., Cheng, G., Zhang, N.B.-M., Castaneda, H., and Ju, L.-K. (2015a) Long-term survival of *Desulfovibrio vulgaris* on carbon steel and associated pitting corrosion. *Corros Sci* **90**: 89–100.
- Chen, M., Xu, P., Zeng, G., Yang, C., Huang, D., and Zhang, J. (2015b) Bioremediation of soils contaminated with polycyclic aromatic hydrocarbons, petroleum, pesticides, chlorophenols and heavy metals by composting: Applications, microbes and future research needs. *Bio-tech Adv* **33**: 745–755.
- Choi, D.-J., You, S.-J., and Kim, J.-G. (2002) Development of an environmentally safe corrosion, scale, and microorganism inhibitor for open recirculating cooling systems. *Mater Sci Eng* **335**: 228–235.
- Cole, J.R., Wang, Q., Fish, J.A., Chai, B., McGarrell, D.M., Sun, Y., *et al.* (2014) Ribosomal Database Project: data and tools for high throughput rRNA analysis. *Nucleic Acids Res* **42**: D633–D642.
- Cord-Ruwisch, R. (1985) A quick method for the determination of dissolved and precipitated sulfides in cultures of sulfate-reducing bacteria. *J Microbiol Methods* **4**: 33–36.
- Dariva, C.G., and Galio, A.F. (2014) Corrosion inhibitors - Principles, mechanisms and applications. In *Developments in Corrosion Protection*. Aliofkhazraei, M. (ed). Rijeka, Croatia: Intech, pp. 365–379.
- Deng, X., Dohmae, N., Nealson, K.H., Hashimoto, K., and Okamoto, A. (2018) Multi-heme cytochromes provide pathway for survival in energy-limited environments. *Sci Adv* **4**: 1–8.
- Deutzmann, J.S., and Spormann, A.M. (2017) Enhanced microbial electrosynthesis by using defined co-cultures. *ISME J* **11**: 704–714.
- Deutzmann, J.S., Sahin, M., and Spormann, A.M. (2015) Extracellular enzymes facilitate electron uptake in biocorrosion and bioelectrosynthesis. *mBio* **6**: 1–8.
- Dinh, H.T., Kuever, J., Mussmann, M., Hassel, A.W., Stratmann, M., and Widdel, F. (2004) Iron corrosion by novel anaerobic microorganisms. *Nature* **427**: 829–832.
- Drønen, K., Roalkvam, I., Beeder, J., Torsvik, T., Steen, I.H., Skauge, A., and Liengen, T. (2014) Modeling of heavy nitrate corrosion in anaerobe aquifer injection water biofilm: a case study in a flow rig. *Environ Sci Technol* **48**: 8627–8635.
- Duncan, K.E., Gieg, L.M., Parisi, V.A., Tanner, R.S., Tringe, S.G., Bristow, J., and Suflita, J.M. (2009) Biocorrosive thermophilic microbial communities in Alaskan north slope oil facilities. *Environ Sci Technol* **43**: 7977–7984.
- Duncan, K.E., Perez-Ibarra, B.M., Jenneman, G., Harris, J.B., Webb, R., and Sublette, K. (2014) The effect of corrosion inhibitors on microbial communities associated with corrosion in a model flow cell system. *Appl Microbiol Biotechnol* **98**: 907–918.
- Enning, D., and Garrelfs, J. (2014) Corrosion of iron by sulfate-reducing bacteria: new views of an old problem. *Appl Environ Microbiol* **80**: 1226–1236.
- Enning, D., Venzlaff, H., Garrelfs, J., Dinh, H.T., Meyer, V., Mayrhofer, K., *et al.* (2012) Marine sulfate-reducing bacteria cause serious corrosion of iron under electroconductive biogenic mineral crust. *Environ Microbiol* **14**: 1772–1787.
- Enning, D., Smith, R., Stolle, J., and Horneman, J. (2016) Evaluating the efficacy of weekly THPS and glutaraldehyde batch treatment to control severe microbial corrosion in a simulated seawater injection system. NACE International Corrosion Conference & Expo Paper no. 7322.
- Garcia, M.T., Campos, E., Sanchez-Leal, J., and Ribosa, I. (1999) Effect of the alkyl chain length on the anaerobic biodegradability and toxicity of quaternary ammonium based surfactants. *Chemosphere* **38**: 3473–3483.
- Hayden, S.C., Chisholm, C., Grudt, R.O., Aguiar, J.A., Mook, W.M., Kotula, P.G., *et al.* (2019) Localized corrosion of low-carbon steel at the nanoscale. *npj Mater Degrad* **3**: 1–9.
- Horsup, D.I., Clark, J.C., Binks, B.P., Fletcher, P.D.I., and Hicks, J.T. (2007) “I put it in, but where does it go?” – The fate of corrosion inhibitors in multiphase systems. NACE International Corrosion Conference & Expo Paper no. 07617.
- Keasler, V., Bennett, B., Bromage, B., Franco, R.J., Lefevre, D., Shafer, J., and Moninuola, B. (2010) Bacterial characterization and biocide qualification for full wellstream crude oil pipelines. NACE International Corrosion Conference & Expo Paper no. 10250.
- Kermani, M.B., and Morshed, A. (2003) Carbon dioxide corrosion in oil and gas production – a compendium. *Corrosion* **59**: 659–683.
- Kotani, T., Kawashima, Y., Yurimoto, H., Kato, N., and Sakai, Y. (2006) Gene structure and regulation of alkane monooxygenase in propane-utilizing *Mycobacterium* sp. TY-6 and *Pseudonocardia* sp. TY-7. *J Biosci Bioeng* **102**: 184–192.
- Lahme, S., Enning, D., Callbeck, C.M., Vega, D.M., Curtis, T.P., Head, I.M., and Hubert, C.R.J. (2019) Metabolites of an oil field sulfide-oxidizing, nitrate-reducing *Sulfurimonas* sp. cause severe corrosion. *Appl Environ Microbiol* **85**: 1–12.
- Lee, W., Lewandowski, Z., Nielsen, P.H., and Hamilton, W.A. (1995) Role of sulfate-reducing bacteria in corrosion of mild steel: a review. *Biofouling* **8**: 165–194.
- Li, G., Gao, P., Wu, Y., Tian, H., Dai, X., Wang, Y., *et al.* (2014) Microbial abundance and community composition influence production performance in a low-temperature petroleum reservoir. *Environ Sci Technol* **48**: 5336–5344.
- Liu, H., Gu, T., Zhang, G., Wang, W., Dong, S., Cheng, Y., and Liu, H. (2016) Corrosion inhibition of carbon steel in CO<sub>2</sub>-containing oilfield produced water in the presence of iron-oxidizing bacteria and inhibitors. *Corros Sci* **105**: 149–160.
- Magot, M., Ollivier, B., and Patel, B.K.C. (2000) Microbiology of petroleum reservoirs. *Antonie Van Leeuwenhoek* **77**: 103–116.
- Migahed, M.A., and Al-Sabagh, A.M. (2009) Beneficial role of surfactants as corrosion inhibitors in petroleum industry: a review article. *Chem Eng Commun* **196**: 1054–1075.
- Mori, K., Tsurumaru, H., and Harayama, S. (2010) Iron corrosion activity of anaerobic hydrogen-consuming microorganisms isolated from oil facilities. *J Biosci Bioeng* **110**: 426–430.

- Nešić, S. (2007) Key issues related to modelling of internal corrosion of oil and gas pipelines – a review. *Corros Sci* **49**: 4308–4338.
- Palmer, J.W., Hedges, W., and Dawson, J.L (eds) (2004) Inhibition concepts and issues. In *The Use of Corrosion Inhibitors in Oil and Gas Production*. London, UK: Manley Publishing, pp. 9–19.
- Pandarínathan, V., Lepková, K., Bailey, S.I., and Gubner, R. (2013) Evaluation of corrosion inhibition at sand-deposited carbon steel in CO<sub>2</sub>-saturated brine. *Corros Sci* **72**: 108–117.
- Quast, C., Pruesse, E., Yilmaz, P., Gerken, J., Schweer, T., Yarza, P., *et al.* (2012) The SILVA ribosomal RNA gene database project: improved data processing and web-based tools. *Nucleic Acids Res* **41**: D590–D596.
- Sanyal, B. (1981) Organic compounds as corrosion inhibitors in different environments - a review. *Prog Org Coat* **9**: 165–236.
- Skovhus, T.L., Eckert, R.B., and Rodrigues, E. (2017) Management and control of microbiologically influenced corrosion (MIC) in the oil and gas industry - overview and a North Sea case study. *J Biotechnol* **256**: 31–45.
- Smith, K.S., and Ingram-Smith, C. (2007) *Methanosaeta*, the forgotten methanogen? *Trends Microbiol* **15**: 150–155.
- Starosvetsky, D., Khaselev, O., Starosvetsky, J., Armon, R., and Yahalom, J. (2000) Effect of iron exposure in SRB media on pitting initiation. *Corros Sci* **42**: 345–359.
- Suzuki, M.T., Taylor, L.T., and DeLong, E.F. (2000) Quantitative analysis of small-subunit rRNA genes in mixed microbial populations via 5'-nuclease assays. *Appl Environ Microbiol* **66**: 4605–4614.
- Tang, H.-Y., Holmes, D.E., Ueki, T., Palacios, P.P., and Lovely, D.R. (2019) Iron corrosion via direct metal-microbe electron transfer. *mBio* **10**: 1–10.
- Tezel, U., and Pavlostathis, S.G. (2015) Quaternary ammonium disinfectants: microbial adaptation, degradation and ecology. *Curr Opin Biotechnol* **33**: 296–304.
- Tezel, U., Pierson, J.A., and Pavlostathis, S.G. (2006) Fate and effect of quaternary ammonium compounds on a mixed methanogenic culture. *Water Res* **40**: 3660–3668.
- Tsurumaru, H., Ito, N., Mori, K., Wakai, S., Uchiyama, T., Iino, T., *et al.* (2018) An extracellular [NiFe] hydrogenase mediating iron corrosion is encoded in a genetically unstable genomic island in *Methanococcus maripaludis*. *Sci Rep* **8**: 1–10.
- Uchiyama, T., Ito, K., Mori, K., Tsurumaru, H., and Harayama, S. (2010) Iron-corroding methanogen isolated from a crude-oil storage tank. *Appl Environ Microbiol* **76**: 1783–1788.
- United States Energy Information Administration (2018) Short-term energy outlook.
- Vera, J.R., Daniels, D., and Achour, M.H. (2012) Under deposit corrosion (UDC) in the oil and gas industry: a review of mechanisms, testing and mitigation. NACE International Corrosion Conference & Expo Paper C2012-0001379.
- Vigneron, A., Alsop, E.B., Chambers, B., Lomans, B.P., Head, I.M., Tsesmetzis, N., and Nojiri, H. (2016) Complementary microorganisms in highly corrosive biofilms from an offshore oil production facility. *Appl Environ Microbiol* **82**: 2545–2554.
- Vigneron, A., Alsop, E.B., Lomans, B.P., Kyripides, N.C., Head, I.M., and Tsesmetzis, N. (2017) Succession in the petroleum reservoir microbiome through an oil field production lifecycle. *ISME J* **11**: 2141–2154.
- Walsh, D., Pope, D., Danford, M., and Huff, T. (1993) The effect of microstructure on microbiologically influenced corrosion. *JOM* **45**: 22–30.
- Wang, L.K., and Langley, D.F. (1975) Determining cationic surfactant concentration. *Ind Eng Chem Prod Res Dev* **14**: 210–212.
- Wessels, S., and Ingmer, H. (2013) Modes of action of three disinfectant active substances: a review. *Regul Toxicol Pharmacol* **67**: 456–467.
- Widdel, F., and Bak, F. (1992) Gram-negative mesophilic sulfate-reducing bacteria. In *The Prokaryotes*. Barlow, A., Trüper, H.G., Dworkin, M., Harder, W., and Schleifer, K.H. (eds). New York: Springer, pp. 3352–3378.
- Widdel, F., and Pfennig, N. (1982) Studies on dissimilatory sulfate-reducing bacteria that decompose fatty acids II. Incomplete oxidation of propionate by *Desulfobulbus propionicus* gen. nov., sp. nov. *Arch Microbiol* **131**: 360–365.
- Yu, Y., Lee, C., Kim, J., and Hwang, S. (2005) Group-specific primer and probe sets to detect methanogenic communities using quantitative real-time polymerase chain reaction. *Biotechnol Bioeng* **89**: 670–679.
- Zhang, C., Cui, F., Zeng, G.M., Jiang, M., Yang, Z.Z., Yu, Z.G., *et al.* (2015) Quaternary ammonium compounds (QACs): A review on occurrence, fate and toxicity in the environment. *Sci Total Environ* **518–519**: 352–362.
- Zhu, Y., Free, M.L., Woollam, R., and Durnie, W. (2017) A review of surfactants as corrosion inhibitors and associated modeling. *Prog Mater Sci* **90**: 159–223.

## Supporting information

Additional supporting information may be found online in the Supporting Information section at the end of the article.

### Appendix S1. Supplementary methods.

**Fig. S1.** Modified 1 l Duran bottle for the study of microbially influenced corrosion (MIC). Bottles are sealed with a gas-tight butyl rubber septum and contain a coupon holder made of electrically insulating polyether ether ketone (PEEK) that houses three carbon steel coupons. The coupon holder is inserted into anaerobic produced water (PW).

**Fig. S2.** Scavenging of corrosion inhibitor (CI) with laboratory-grade sand (SiO<sub>2</sub>). Sterilized sand (15% wt/wt) was added to glass bottles containing sterile anoxic produced water medium ( $n = 2$ ). Following addition of 3 mg Cl l<sup>-1</sup>, Cl concentration was monitored over 14 days. Cl concentration in sterile control tests without sand ( $n = 2$ ) is shown for comparison.

**Fig. S3.** Surface depth profiles of carbon steel coupons incubated in oily produced water for 15 months. Coupons incubated in sand-free bottles ( $n = 4$ ) showed no signs of corrosion and remained virtually pristine, which was attributed to higher concentrations of residual CI. Addition of sand lowered CI concentrations in the other set of produced water incubations ( $n = 5$ ) and highly localized corrosion,

denoted using white arrows, was observed on most of the coupons under these conditions. Scale bar = 1 cm.

**Fig. S4.** Quantification of planktonic microorganisms in long-term produced water and synthetic produced water incubations with carbon steel coupons. The sum of archaeal and bacterial 16S rRNA gene copies per ml of (A) produced water is shown for incubations with ( $n = 4$ ) and without ( $n = 5$ ) sand at test take-down after 15 months and of (B) synthetic produced water incubations with 0, 3, 5 and 10 mg Cl<sup>-1</sup> ( $n = 3$ ) at test take-down after 3 months.

**Fig. S5.** Inhibition of (A) sulfidogenesis, and (B) methanogenesis by corrosion inhibitors (CIs) in synthetic produced water medium inoculated with 1% (vol/vol) of an oil field enrichment culture. Formation of sulfide and methane is shown in duplicate cultures without CI (circles), with 3 mg Cl<sup>-1</sup> (squares) and with 10 mg Cl<sup>-1</sup> (triangles).

**Fig. S6.** Surface depth profiles of carbon steel coupons incubated in synthetic produced water medium for 3 months. Different concentrations of corrosion inhibitor (CI) were added to triplicate cultures containing oil field microorganisms and one coupon each. One sterile control was set up per CI concentration tested. Scale bar = 2.5 cm, white arrows denote localized corrosion features.

**Fig. S7.** Hydrogen concentration in 1.6 l microcosms containing synthetic produced water medium and a carbon steel coupon. (A) Hydrogen formation and consumption in microcosms inoculated with an oil field enrichment culture, amended with 3 mg Cl<sup>-1</sup> (squares), 5 mg Cl<sup>-1</sup> (triangles) or 10 mg Cl<sup>-1</sup> (diamonds). CI-free cultures (circles) were included as controls. Error bars represent standard error of the mean between biological triplicates. (B) Hydrogen formation in sterile control microcosms ( $n = 1$ ).

**Fig. S8.** (A–D) Impact of corrosion inhibitors (CI) on the activity of oil field microorganisms grown in microcosms with synthetic produced water medium. Microcosms ( $n = 3$ ) containing carbon steel coupons were amended with 0 mg Cl<sup>-1</sup> (circles), 3 mg Cl<sup>-1</sup> (squares), 5 mg Cl<sup>-1</sup> (triangles) or 10 mg Cl<sup>-1</sup> (diamonds) and incubated for 3 months. (E–H) Sterile control microcosms ( $n = 1$ ).

**Fig. S9.** Steel-attached biofilm and planktonic microbial communities in anoxic microcosms with synthetic produced water medium and carbon steel coupons. Microcosms ( $n = 3$ ) were amended with 0 mg Cl<sup>-1</sup>, 3 mg Cl<sup>-1</sup>, 5 mg Cl<sup>-1</sup> or 10 mg Cl<sup>-1</sup> and incubated for 3 months. (A) Sessile bacterial and archaeal microbial community composition of biofilms collected from steel coupons. (B) Planktonic bacterial and archaeal microbial community composition in microcosm produced waters. (A) and (B) depict families which account for  $\geq 2.5\%$  of total reads (average of biological replicates) in at least one of the four data sets (0, 3, 5 or 10 mg Cl<sup>-1</sup>).

**Fig. S10.** (A) Concentration of corrosion inhibitor (CI) in iron-free incubations containing synthetic produced water medium (SPWM). CI was added at 3 mg l<sup>-1</sup> to triplicate bottles containing either sulfide-free sterile SPWM (crosses), sterile SPWM with 0.8 mM Na<sub>2</sub>S (diamonds), a heat-sterilized sulfidic culture (triangles), or an active sulfidic culture (circles). (B) Dissolved sulfide in incubations of SPWM.

**Fig. S11.** Microbially influenced decrease in corrosion inhibitor (CI) concentration in aerobic artificial seawater medium (600 ml) with 0.5 g of coastal sediment. Inhibitor was added at 25 mg Cl<sup>-1</sup> to both, aerobic and anaerobic cultures. Sterile controls were obtained through heat-sterilization of medium containing sediment, prior to addition of CI.

**Fig. S12.** Concentration of the quaternary ammonium compounds (QAC) benzyltrimethyl-n-dodecylammonium chloride (a C12-QAC) and benzyltrimethyl-n-hexadecylammonium chloride (a C16-QAC) in synthetic produced water medium containing oil field microorganisms and carbon steel coupons (A and B). QAC concentrations in abiotic controls are also shown. (C) Surface depth profile of carbon steel coupons exposed to produced water medium for 2 months. Scale bar = 2.5 cm, white arrow and dashed circle denote localized corrosion features.

**Table S1.** Raw data used to calculate weight loss corrosion rates.

**Table S2.** Chemical composition and qPCR assay results of the West African produced water.